

1 **Technical Note: VUV photodesorption rates from water ice in the**
2 **120-150 K temperature range – Significance for Noctilucent Clouds**

3
4 M. Yu. Kulikov¹, A. M. Feigin¹, S. K. Ignatov², P. G. Sennikov^{3,1}, Th. Bluszcz⁴,
5 and O. Schrems⁴

6
7 ¹ Institute of Applied Physics of the Russian Academy of Science, 46 Ulyanov Str.,
8 603950, Nizhny Novgorod, Russia

9 ² Lobachevsky State University of Nizhny Novgorod, 23 Gagarin Ave., 603950,
10 Nizhny Novgorod, Russia

11 ³ Institute of Chemistry of High-Purity Substances of the Russian Academy of
12 Sciences, 49 Tropinin St., 603950, Nizhny Novgorod, Russia

13 ⁴ Alfred Wegener Institute for Polar and Marine Research, Am Handelshafen 12,
14 D-27570 Bremerhaven, Germany

15 Correspondence to: M. Yu. Kulikov (kulm@appl.sci-nnov.ru)

16
17 **Abstract**

18 Laboratory studies have been carried out with the aim to improve our understanding
19 of physicochemical processes which take place at the water ice/air interface initiated
20 by solar irradiation with a wavelength of 121.6 nm. It was intended to mimic the
21 processes of ice particles characteristic of Noctilucent Clouds (NLCs). The
22 experimental set-up used includes a high-vacuum chamber, a gas handling system, a
23 cryostat with temperature controller, an FTIR spectrometer, a vacuum ultraviolet
24 hydrogen lamp, and a microwave generator. We report the first results of
25 measurements of the absolute photodesorption rate (loss of substance due to the
26 escape of photoproducts into gas phase) from thin (20-100 nm) water ice samples
27 kept in the temperature range of 120-150 K. The obtained results show that a flow of
28 photoproducts into the gas phase is considerably lower than presumed in the recent
29 study by Murray and Plane (2005). The experiments indicate that almost all

30 photoproducts remain in the solid phase, and the principal chemical reaction between
31 them is the recombination reaction $H+OH \rightarrow H_2O$ which is evidently very fast. This
32 means that direct photolysis of mesospheric ice particles seems to have no
33 significant impact on the gas phase chemistry of the upper mesosphere.

34

35 **1 Introduction**

36 Noctilucent Clouds (NLCs) are the highest clouds of the Earth's atmosphere. They
37 are formed during summer at middle to high latitudes in an altitude range between 80
38 and 90 km when the air temperature drops below 150 K (Gadsden and Schröder,
39 1989; Thomas, 1991; Lübken, 1999). NLC features are important and sensitive
40 indicators of global climate change, anthropogenic influence on atmospheric
41 composition, and dynamical processes in the mesosphere – lower thermosphere
42 altitudes. Seasonal and spatial occurrence zones of NLCs are in a good correlation
43 with particularities of the so-called polar mesosphere summer echoes (Thomas et al.,
44 1989; Thayer et al., 2003; von Zahn and Berger, 2003). In spite of the fact that the
45 clouds were already discovered in the nineteenth century (Jesse, 1885), many
46 processes of their formation and spatiotemporal evolution are still poorly understood
47 because NLCs are rather far away from both, the ground-based and satellite
48 instruments of atmospheric sounding. Only recently, Hervig et al. (2001) presented
49 the first direct experimental confirmation of Alfred Wegener's idea (1912) that
50 particles of NLCs consist primarily of water ice and are formed as a result of water
51 vapour condensation¹.

52 It is well known that water vapour is one of the most important trace gases of the
53 upper mesosphere (e.g., Brasseur and Solomon, 1986). In particular, the
54 photodissociation of water vapour by solar ultraviolet radiation with the wavelength of
55 121.6 nm (known as the Lyman- α line) is the principal source for the family of odd
56 hydrogen ($HO_x = H + OH + HO_2$). Gas-phase reactions with participation of these
57 components represent the main sink for the components of the family of odd oxygen
58 ($O_x = O(^1D) + O(^3P) + O_3$). Therefore, as water vapour concentration grows, daily
59 concentration of O_x decreases and *vice versa*. Recently, Murray and Plane (2005)
60 noticed that photolysis of H_2O molecules contained in the solid phase also takes

¹ For more details about the history of the discovery and investigations of NLCs please see reviews by Gadsden and Schröder (1989) and Thomas (1991).

61 place and showed that photochemical processes with participation of NLC particles,
62 may in principle influence the chemistry of the upper mesosphere as an additional
63 source of HO_x. Indeed, the solar Lyman- α photons penetrate into particles of NLCs
64 and are absorbed essentially by H₂O molecules of the ice particles having typical
65 mean radii of some tens nm (e.g., von Cossart et al., 1999)) comparable with the
66 attenuation depth (~45 nm (Warren, 1984)) of 10.2 eV photons in water ice.
67 Moreover, the calculations by Murray and Plane showed that Mie absorption
68 efficiency at 121.6 nm for spherical ice particles with radii larger than 30 nm is close
69 to unity. The products (H and OH) of the photolysis of water ice may volatilise leading
70 to an enhancement of HO_x concentration in the gas phase with a corresponding
71 increase in O_x removal. Murray and Plane (2005) performed numerical analyses of
72 the impact of ice photolysis on the evolution of O concentration distribution in the
73 upper summer mesosphere, assuming a realistic distribution of ice particles. It was
74 shown that the effect is insignificant at night (because there is no irradiation) and is
75 most pronounced during daytime when O concentration may decrease (relative to the
76 unperturbed level) several fold at the heights of cloud existence. However, in this
77 model study Murray and Plane considered the upper limit of photodesorption rates
78 from particles of NLCs according to which each Lyman- α photon absorbed by a
79 H₂O molecule in the ice results in the immediate ejection of one H atom and one OH
80 radical into gas phase. Therefore, these authors justly pointed out the need of
81 laboratory measurements of H and OH yield from a thin ice film or another analog of
82 small ice particles under temperatures pertinent to the summer mesosphere. It
83 should be noted that release of these photoproducts (and some others: H₂, O(³P),
84 O(¹D), H₂O) from VUV (157 and 193 nm) irradiated water ice at high temperatures
85 (90-140 K) were directly observed in the works by Yabushita et al. (2008a, 2008b)
86 and Hama et al. (2009a, 2009b, 2009c, 2010). However, these studies do not provide
87 information about quantum yields of photoproducts and, therefore, do not give an
88 answer to the question addressed by Murray and Plane (2005). Before these works,
89 Westley et al. (1995a, 1995b) measured desorption of photoproducts during Lyman -
90 α irradiation of thick (500nm) water ice samples at T=35–100 K by using a quartz
91 crystal resonator microbalance and mass - spectroscopy. They found out that most of
92 the desorbed species were water molecules and values of photodesorption yield Y₀
93 (number of H₂O molecules desorbed per incident photon) were essentially less than
94 1 molecule/photon. In particular, the maximal value of Y₀~8·10⁻³molecule/photon

95 obtained at $T=100\text{K}$ corresponded approximately to the probability of desorption from
96 the topside molecular layer of the ice. Watanabe et al. (2000) carried out mass -
97 spectroscopy experiments on the formation of D_2 molecules from amorphous thin
98 (thickness 4 and 12 nm) D_2O ice samples by VUV irradiation (126 and 172 nm) at 12
99 K. According to their results, only a small fraction of the total D_2 photoproducts was
100 released into gas-phase at the low temperature. Also they determined the cross
101 section for the photodestruction of D_2O which was found out to be close to the results
102 gotten by Westley et al. (1995a, 1995b) for water ice.

103 This note reports results of the first measurements of the absolute photodesorption
104 rate (loss of substance due to the escape of photoproducts into gas phase) from thin
105 (20-100 nm) water ice samples in the temperature range of 120-150 K.

106

107 **2. Experimental details**

108

109 **2.1. Apparatus**

110 The experimental set-up consists of a closed-cycle He refrigerator (Leybold ROK 10-
111 300) and a Fourier Transform Infrared Spectrometer (Bruker IFS 66v)). The
112 apparatus comprises a high-vacuum chamber with a volume of about 2000 cm^3 (Fig.
113 1) pumped continuously by a turbomolecular pump system (Leybold-Heraeus)
114 securing high vacuum in the chamber down to the 10^{-8} mbar range. Inside the
115 chamber at the cold end of the cryostat there is a vertically mounted aluminium mirror
116 (2.5 x 4 cm in size) as a substrate whose temperature is precisely regulated by a
117 temperature controller (Lake Shore, model 340). The temperature can be selected in
118 the 10-300 K range. The oxygen (Air Liquide 5.5 (≥ 99.9995 Vol%)) or water samples
119 are deposited onto the cold mirror by means of a gas-inlet system equipped with
120 needle valves which allow controlling the deposition rate. The upper part of the high
121 vacuum chamber has three ports, two of which are equipped with MgF_2 (5 mm thick)
122 input and output windows for the VUV lamp. The third port has a KBr window for the
123 IR beam of the FTIR spectrometer. The input for the VUV lamp is placed with an
124 angle of incidence $\sim 45^\circ$ to the mirror surface and, according to the estimates of the
125 manufacturer, MgF_2 transmits about 60% of the quantum flux at the wavelength of
126 121.6 nm. As a VUV source (Lyman- α) we use a resonance hydrogen lamp (Ophos
127 Instruments) containing a mixture of 10% H_2 and 90% Ar, which is excited by a

128 microwave generator (Ophos Instruments, model MPG-4M) with a frequency of
129 2450 MHz. The intensity of the lamp is determined by the power supplied by the
130 microwave generator. The FTIR spectrometer is placed on rails allowing precise
131 positioning of the instrument with respect to the cryostat with the sample. This is
132 important in order to achieve a good overlap of the areas of the light spots from both,
133 infrared (from spectrometer light source) and vacuum ultraviolet irradiation (from VUV
134 lamp) of the ice film sample on the substrate. The overlap can be checked through
135 the windows in the vacuum chamber. The operation of the FTIR spectrometer is PC
136 controlled by means of software (OPUS) that permits scanning spectra over a wide
137 range (from 6000 to 500 cm^{-1}) and analyzing the obtained spectra. The spectra are
138 recorded with a spectral resolution of 0.2 cm^{-1} in the RAIRS mode (reflection
139 absorption infrared spectroscopy) where the IR beam passes through the sample
140 twice (see Fig.1).

141

142 **2.2. Experimental procedures**

143 Every experiment with a particular sample of ice was conducted in two stages. At the
144 first stage, a fixed mirror temperature was set by means of the temperature controller
145 and the background spectrum was recorded. Then, an ice film was prepared by
146 depositing water vapour onto the mirror. Velocity of the deposition and sample
147 thickness were controlled by a needle valve of the gas-inlet system and by tracking
148 the evolution of absorption bands in the FTIR spectra. Thickness and structure of the
149 ice sample were monitored with the FTIR spectrometer using available data on
150 intensities of OH stretching bands of water ice in the 3600-3000 cm^{-1} range. We
151 prepared thin ice samples with characteristic thicknesses of 20-100 nm, which
152 correspond to typical radii of NLC particles (e.g., von Cossart et al., 1999). The time
153 of individual sample deposition varied within 1-3 min. After that, several IR spectra of
154 unirradiated ice were recorded. In spite of the relatively fast velocity of deposition, the
155 main features of these spectra demonstrated that all samples were crystalline (cubic)
156 ice. It should be noted, that direct IR scanning of NLCs carried out by the ACE-FTS
157 satellite instrument also showed that cloud particles were composed of crystalline ice
158 (Eremenko et al., 2005).

159 At the second stage, the vacuum ultraviolet lamp was switched on and the ice films
160 were exposed to VUV radiation. After each photolysis IR spectra of the irradiated ice

161 films were recorded. Comparison of these spectra with the spectra obtained before
162 irradiation allowed analyzing the influence of vacuum ultraviolet radiation on the
163 water ice samples.

164

165 **2.3. Calibration of the hydrogen discharge lamp**

166 It is well known that the ultraviolet flux given by a microwave powered discharge lamp
167 strongly depends on the operating conditions and can vary in the 10^{12} - 10^{15} photons
168 $\text{cm}^{-2}\text{s}^{-1}$ range (Leto and Baratta, 2003). Based on this, we performed a series of
169 measurements of the absolute magnitude of the flux of Lyman- α photons that reach
170 the ice sample at different adjustments of the microwave generator power. For this
171 procedure we applied the “ozone method” (e.g., Gerakines et al., 2000, Leto and
172 Baratta, 2003; Schriver et al., 2004). The intensity of the lamp was determined by
173 measuring the $\text{O}_2 \rightarrow \text{O}_3$ conversion rate in a VUV photolyzed sample of solid O_2 at
174 16 K. For ensuring absorption by the sample of almost all incoming Lyman- α
175 photons we prepared O_2 layers with a thicknesses of about 1-2 μm .

176 The ozone formation as a function of photolysis time was monitored with the FTIR
177 spectrometer via the ν_3 absorption band at about 1040 cm^{-1} . Appearance of new
178 narrow absorption lines near 1040 cm^{-1} soon after the beginning of irradiation signals
179 formation of ozone (see Fig. 2), and growth of the amplitude of this bands with time is
180 a consequence of the increase of the concentration of this constituent. The observed
181 ozone absorption band at about 1040 cm^{-1} has a complex fine structure with several
182 maxima (see Fig. 2). One can see 8 pronounced maxima (1042 cm^{-1} , 1039.8 cm^{-1} ,
183 1037.7 cm^{-1} , 1034.3 cm^{-1} , 1032.6 cm^{-1} , 1031.1 cm^{-1} , 1030.2 cm^{-1} , and 1029.6 cm^{-1})
184 and 5 comparatively weak maxima. The positions of all the 13 maxima and their
185 amplitude ratio are independent of the generator power and duration of irradiation.
186 Dyer et al. (1997) in their work analysed the ozone absorption line arising in a sample
187 of solid molecular oxygen as a result of laser irradiation with variable wavelength in
188 the range 210-250 nm and they showed that the appearance of the complex
189 structure of ozone absorption band is associated with the formation of ozone
190 dimmers. However, different trapping sites of the ozone species within the lattice of
191 solid oxygen have to be considered as well.

192 For finding the radiation intensity of the lamp for a specific generator power we made
193 a series of successive measurements of the integrated area of the 1040 cm^{-1}
194 absorption band multiplet (S) as a function of irradiation time. After that, the lamp
195 intensity was determined from the following relation

$$196 \quad I = \frac{dS}{dt} / (Y \cdot S_0),$$

197 where the derivative $\frac{dS}{dt}$ is found by the linear part of the function S(t). Y is the
198 quantum yield for the formation of O_3 from O_2 , and S_0 is the intensity of the ozone
199 bands at 1040 cm^{-1} . The value of $Y \cdot S_0$ was adopted from the study of Cottin et al.
200 (2003) and is equal to $8.4 \cdot 10^{-18}\text{ cm} \cdot \text{photon}^{-1}$. Our measurements enabled us to
201 ascertain that, depending on the generator output power (4-100 W), the photon flux
202 intensity varies within the range $5 \cdot 10^{12} - 10^{14}\text{ photons cm}^{-2}\text{s}^{-1}$. For a power less than
203 4 W, discharge generation in a VUV lamp becomes unstable.

204

205 **3. Measurements of the photodesorption rates from thin water ice samples**

206 The experiments and further analysis of the results were carried out under the
207 following assumptions:

208 1. The column density of thin (20-100 nm) samples of water ice films is related
209 linearly to the integrated area of the band with a maximum at about 3275 cm^{-1}
210 (hereinafter S) of the IR absorption of water ice. The intensity of the absorption band
211 (hereinafter S_0) is known from the literature (Allamandola et al., 1988). No phase
212 transition of water ice samples to hexagonal or amorphous ice was registered during
213 irradiation, as was found, for example, by Leto and Baratta (2003). So, the value of
214 S_0 can be considered to be constant. Therefore, by successive measurements of the
215 principal absorption band of water it is possible to control the magnitude of the
216 column density $N = S/S_0$. For example, for the ice sample thickness of 100 nm, $N \sim$
217 $3 \cdot 10^{17}\text{ molecules/cm}^2$, $S \sim 60\text{ cm}^{-1}$.

218 2. Additional uncontrolled condensation of H_2O molecules on the mirror occurs (H_2O
219 desorption from the warmer walls of the vacuum chamber) during the lifetime of an
220 ice sample at high temperatures (120-150 K), giving rise to monotonic increase of the
221 values of S and N.

222 3. As follows from the results of laboratory studies of low-temperature (10-20 K) ice
223 photolysis, Lyman- α irradiation causes a wide spectrum of physical and chemical
224 processes in the ice (Gerakines et al., 1996; Schriver et al., 2004). Firstly, the
225 reaction $\text{H}_2\text{O} + h\nu$ (121.6 nm) may have an additional channel $\text{H}_2 + \text{O}$. Secondly,
226 chemical reactions with formation of secondary products H_2O , HO_2 , HO_3 , H_2O_2 , O_2 ,
227 O_3 can take place between the primary photolysis products. Thirdly, the mobility of
228 the photoproducts inside the ice (and, correspondingly, their conversion to gas
229 phase) is determined by diffusion whose coefficient strongly depends on the chemical
230 composition of the species and the temperature. At relatively high temperatures of
231 order 100 K and higher, nearly all primary and secondary photoproducts (except H_2O
232 and H_2O_2) are extremely mobile. Specifically, the value of atomic hydrogen diffusivity
233 D_{H} in water ice at temperatures of 120-150 K varies within the $\sim 10^{-12}$ - 10^{-11} m^2/s
234 range (Bartels et al., 1992). The diffusion time for the escape of this photoproduct
235 into the gas phase from an ice sample with thickness $L = 100$ nm is readily estimated
236 to be $L^2 \cdot D_{\text{H}}^{-1} \sim 10^{-3}$ - 10^{-2} s. Thus, considering that hydrogen peroxide formation is a
237 relatively slow process even at high temperatures, we come to the following
238 conclusions:

239
240 Firstly, recovery of H_2O molecules (primarily as a result of $\text{H}+\text{OH}$ recombination) is
241 the basic process limiting the rate of photodesorption from water ice samples.
242 Secondly, irreversible photodissociation of water molecules in irradiated ice will lead
243 to a proportional decrease of the integrated area of the 3275 cm^{-1} band, so that the
244 rate of column density decrease under exposure to VUV radiation will correlate with
245 the rate of photodesorption from the water ice sample. In particular, in the case
246 addressed by Murray and Plane (2005), absorption of a definite amount of Lyman- α
247 photons over a certain period of irradiation leads to the same change of column
248 density.

249 In accord with the above enumerated observations, each experiment with a separate
250 sample at a specific temperature (in the 120-150 K intervals) was carried out in two
251 stages. At the first stage, a thin sample was formed, after which its IR spectrum was
252 regularly recorded without irradiation for quite a long time (about two hours). This
253 enables determining the rate of the uncontrolled growth of column density. At the
254 second stage, the VUV lamp was turned on and IR spectra were recorded repeatedly
255 over a long time interval. The irradiation was performed at maximum generator

256 power, so that the lamp intensity I was about $6 \cdot 10^{15}$ photons $\text{cm}^{-2} \cdot \text{min}^{-1}$ in all the
257 experiments. Thus, if photodesorption is an essential process (the absolute
258 photodesorption yield $Y_0 \sim 1$ molecule/photon), then the lifetime of thin (20-100 nm)
259 water ice samples should not be longer than 50-100 min. At least, we expected to
260 obtain a break of the time curve of column density when starting VUV irradiation.

261 Nevertheless, the conducted experiments demonstrated that the photodesorption
262 rates from thin water ice samples were very small for all values of temperature in the
263 120-150 K interval (see Fig.3). All the obtained functions $N(t)$ were monotonic,
264 without pronounced breaks at the start of irradiation. Average (over one experiment)
265 values of column density growth rates dN/dt were much less than the lamp intensity,
266 indicating that the absolute photodesorption yield Y_0 must be much less than 1
267 molecule/photon. At $T=130$ K, the rate of uncontrolled growth of sample thickness is
268 $\sim 1.5 \cdot 10^{15}$ molecules $\text{cm}^{-2} \cdot \text{min}^{-1}$, whereas at higher temperature ($T=150$ K) the
269 average value of this rate is still lower: $\sim 8.6 \cdot 10^{14}$ molecules $\text{cm}^{-2} \cdot \text{min}^{-1}$. The absence
270 of a break in $N(t)$ gives the following estimate for the absolute photodesorption yield

271 $Y_0 \ll dN/dt \cdot I^{-1}$, from which follows that in the presented examples
272 $Y_0 \ll 0.25$ molecule/photon at 130 K and $Y_0 \ll 0.14$ molecule/photon at 150 K.
273 Moreover, the presented plots include the asymptotic trends of the column density
274 corresponding to different theoretical values of absolute photodesorption yield. To
275 compare the trends with experimental behaviour of the column density it can be
276 concluded that real experimental values of Y_0 are essentially less than 0.05-
277 0.1 molecule/photon in both cases.

278

279 **4. Discussion and Conclusion**

280 The conducted experiments demonstrate that retrieval of H_2O molecules almost fully
281 suppresses photodesorption from a thin water ice sample at the temperatures of 120-
282 150 K. The absorption cross-section (σ) of Lyman- α of photons in ice is known to
283 be $\sim 8 \cdot 10^{-18}$ cm^2 (Westley et al, 1995a) and is only weakly temperature dependent.
284 Therefore, the characteristic time of VUV photodissociation of a specific water
285 molecule (and hence, formation of H and OH products at this point) with the lamp
286 intensity $I=10^{14}$ photons $\text{cm}^{-2} \cdot \text{s}^{-1}$ may be assessed to be $\tau \geq (\sigma I)^{-1} \sim 10^3$ s. Note that
287 this time is at least 5-6 orders of magnitude higher than the diffusion time of atomic
288 hydrogen escaping into gas phase (see § 3). Consequently, for the explanation of the

289 results obtained we can assume that H₂O molecules are retrieved within the bulk
290 mainly as a result of H+OH recombination reaction that follows immediately after
291 photodissociation of H₂O, so that photoproducts do not have sufficient time to escape
292 from the lattice site where they were born. However, directly at the surfaces of the ice
293 particles the situation might be different due to different intermolecular hydrogen
294 bonding interactions (Ignatov et al., 2009).

295 Note that under real mesopause conditions, the intensity of the Lyman- α radiation is
296 approximately $(2-6) \cdot 10^{11}$ photons cm⁻²s⁻¹, depending on the height and solar activity,
297 which is more than two orders of magnitude lower than the intensity of our hydrogen
298 lamp. Thus, summarizing of the obtained results leads to the conclusion that
299 photodesorption from NLCs particles seems to be an absolutely insignificant process
300 in the photochemistry of the upper mesosphere. Almost all the photoproducts are
301 expected to remain in the solid phase after photolysis, and the principal chemical
302 reaction between them is the recombination H+OH->H₂O which is evidently very fast.

303

304 **Acknowledgements**

305 The work was performed with support by the DAAD (German Academic Exchange
306 Service) with the fellowship (study visits) and eastpartnership programmes as well as
307 by the RFBR (project 10-05-01112).

308

309 **References**

310 Allamandola, L. J., Sandford, S. A. and Valero, G. J.: Photochemical and Thermal
311 Evolution of Interstellar/Precometary Ice Analogs, *Icarus*, 76, 225-252, 1988.

312 Bartels, D. M., Han, P. and Percival, P. W.: Diffusion and CIDEP of H and D atoms in
313 solid H₂O, D₂O and isotopic mixtures, *Chem. Phys.*, 164, 421-437, 1992.

314 Brasseur, G. and Solomon, S.: *Aeronomy of the Middle Atmosphere*, 452 pp., D.
315 Reidel, Norwell, Mass., 1986.

316 Cottin, H., Moore, M. H. and Bénilan, Y.: Photodestruction of relevant interstellar
317 molecules in ice mixtures, *Astroph. J.*, 590, 874-881, 2003.

318 Dyer, M. J., Bressler, C. G., Copeland, R. A.: Photodissociation of solid oxygen with
319 tunable ultraviolet laser light: ozone production monitored via Fourier-transform
320 infrared spectroscopy, *Chem. Phys. Lett.*, 266, 548-553, 1997.

321 Eremenko, M. N., Petelina, S. V., Zsetsky, A. Y., Karlsson, B., Rinsland, C. P.,

322 Llewellyn, E. J., Sloan, J. J.: Shape and composition of PMC particles derived from
323 satellite remote sensing measurements Geophys. Res. Lett., 32, L16S06,
324 doi:10.1029/2005GL023013, 2005.

325 Gadsden, M. and Schröder, W.: Noctilucent clouds, Springer Verlag, Berlin, 1989.

326 Gerakines, P. A., Schutte, W. A., Ehrenfreund, P.: Ultraviolet processing in
327 interstellar ice analogs. 1. Pure ices, A&A, 312, 289-305, 1996.

328 Gerakines, P. A., Moore, M. H., and Hudson, R. L.: Carbonic acid production in H₂O :
329 CO₂ ices - UV photolysis vs. proton bombardment, A&A, 357, 793-800, 2000.

330 Hama, T., Yokoyama, M., Yabushita, A., Kawasaki, M., Andersson, S.: Desorption of
331 hydroxyl radicals in the vacuum ultraviolet photolysis of amorphous solid water at 90
332 K, J. Chem. Phys., 131, 054508, 2009a.

333 Hama, T., Yabushita, A., Yokoyama, M., Kawasaki, M., and Watanabe, N.: Formation
334 mechanisms of oxygen atoms in the O(¹D₂) state from the 157 nm photoirradiation of
335 amorphous water ice at 90 K, J. Chem. Phys., 131, 114510, 2009b.

336 Hama, T., Yabushita, A., Yokoyama, M., Kawasaki, M., and Watanabe, N.: Formation
337 mechanisms of oxygen atoms in the O(³P_J) state from the 157 nm photoirradiation of
338 amorphous water ice at 90 K, J. Chem. Phys., 131, 114511, 2009c.

339 Hama, T., Yokoyama, M., Yabushita, A., Kawasaki, M., Andersson, S., Western, C.
340 M., Ashfold, M. N. R., Dixon, R. N., and Watanabe, N.: A desorption mechanism of
341 water following vacuum-ultraviolet irradiation on amorphous solid water at 90 K, J.
342 Chem. Phys., 132, 164508, 2010.

343 Hervig, M., Thompson, E., McHugh, M., Gordley, L., Russell III, J., and Summers, M.
344 E.: First confirmation that water ice is the primary component of polar mesospheric
345 clouds, Geophys. Res. Lett., 28, 971–974, 2001.

346 Ignatov, S. K., Razuvaev, A. G., Sennikov, P. G. and Schrems, O.: H₂O₂ adsorption
347 on the ice *1h* surface. Theoretical study with systematic assessment of the orientation
348 isomerism of the hydrogen bond network, J. Mol. Struct. THEOCHEM, 908, 47-54,
349 2009.

350 Jesse, O.: Auffallende Abenderscheinungen am Himmel, Meteorol. Z., 2, 311-312,
351 1885.

352 Leto, G. and Baratta, G.A.: Ly- α photon induced amorphization of I_c water ice at 16
353 Kelvin Effects and quantitative comparison with ion irradiation, A&A, 397, 7–13,
354 2003.

355 Lübken, F.J.: Thermal structure of the Arctic summer mesosphere, J. Geophys. Res.-

356 Atmos., 104, 9135–9149, 1999.

357 Murray, B. J. and Plane, J. M. C.: Modelling the impact of noctilucent cloud formation
358 on atomic oxygen and other minor constituents of the summer mesosphere, Atmos.
359 Chem. Phys., 5, 1027–1038, 2005.

360 Schriver, A., Coanga, J. M., Schriver-Mazzuoli, L., and Ehrenfreund, P.: FTIR studies
361 of ultraviolet photo-dissociation at 10 K of dimethyl ether in argon and nitrogen
362 matrices, in the solid phase and in amorphous water ice, Chem. Phys. Lett., 386,
363 377–383, 2004.

364 Thayer, J. P., G. E. Thomas, and F.-J. Lübken: Foreword: Layered phenomena in the
365 mesopause region, J. Geophys. Res., 108(D8), 8434, doi:10.1029/2002JD003295,
366 2003.

367 Thomas, G. E.: Mesospheric clouds and the physics of the mesopause region, Rev.
368 Geophys., 29, 553–575, 1991.

369 Thomas, G. E., Olivero, J. J. , Jensen, E. J. , Schröder, W. , and Toon O. B.: Relation
370 between increasing methane and the presence of ice clouds at the mesopause,
371 Nature, 338, 490–492, 1989.

372 von Cossart, G., Fiedler, J.; and von Zahn, U.: Size distributions of NLC particles as
373 determined from 3-color observations of NLC by ground-based lidar, Geophys. Res.
374 Lett., 26, 1513-15 16, 1999.

375 von Zahn, U. and Berger, U.: Persistent ice cloud in the midsummer upper
376 mesosphere at high latitudes: Three-dimensional modeling and cloud interactions
377 with ambient water vapor, J. Geophys. Res.-Atmos., 108, art. no. 8451,
378 doi:10.1029/2002JD002409, 2003.

379 Warren, S.: Optical constants of ice from the ultraviolet to the microwave, Appl. Opt.,
380 23, 1206–1225, 1984.

381 Watanabe, N., Horii, T., and Kouchi, A.: Measurements of D₂ yields from amorphous
382 D₂O ice by ultraviolet irradiation at 12K, Astrophys. J., 541, 772–778, 2000.

383 Wegener, A.: Die Erforschung der obersten Atmosphärenschichten, Gerlands Beitr.
384 Geophys., 11, 102, 1912.

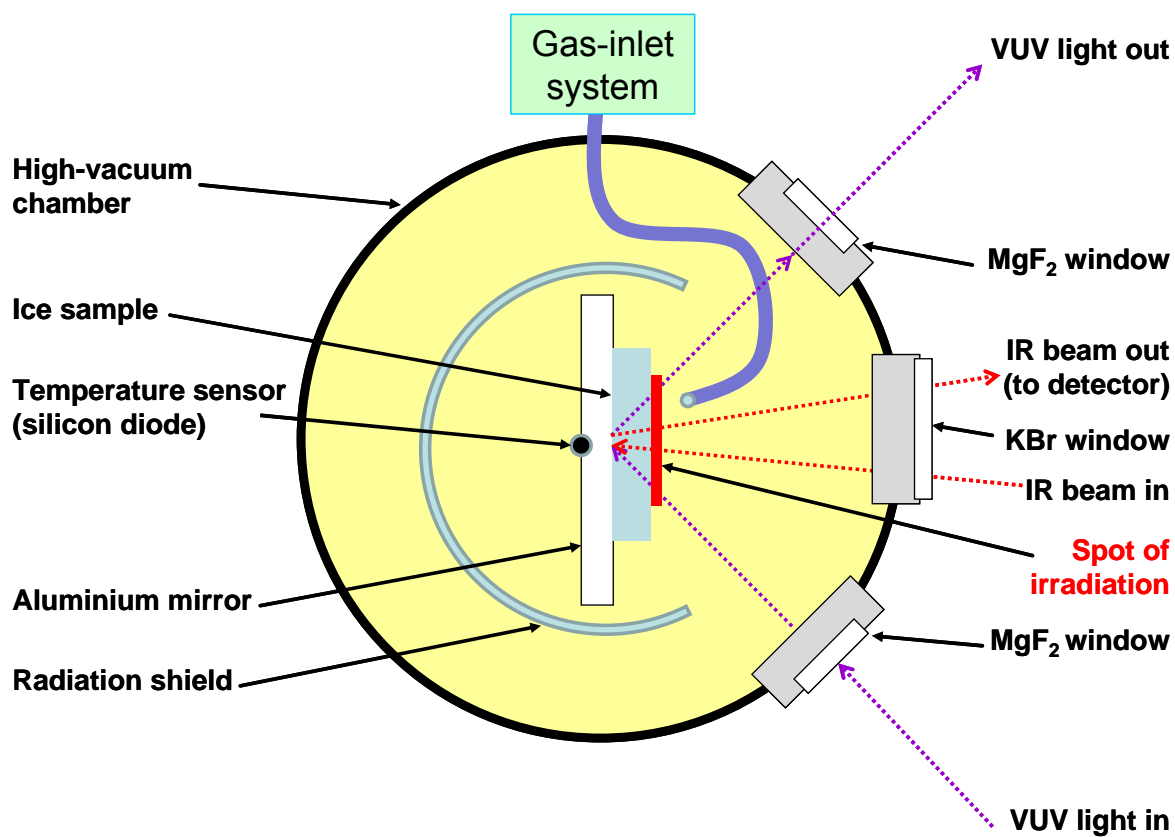
385 Westley, M. S., Baragiola, R. A., Johnson, R. E., and Baratta, G. A.: Ultraviolet
386 photodesorption from water ice, Planet. Space Sci., 43(10/11), 1311-1315, 1995a.

387 Westley, M. S., Baragiola, R. A., Johnson, R. E., and Baratta, G. A.: Photodesorption
388 from low-temperature water ice in interstellar and circumsolar grains, Nature, 373,
389 405–407, 1995b.

390 Yabushita, A., Hama, T., Iida, D., Kawanaka, N., Kawasaki, M., Watanabe, N.,
391 Ashfold, M. N. R., and Looock, H.-P.: Release of hydrogen molecules from the
392 photodissociation of amorphous solid water and polycrystalline ice at 157 and 193
393 nm, *J. Chem. Phys.*, 129, 044501, 2008a.

394 Yabushita, A., Hama, T., Iida, D., Kawanaka, N., Kawasaki, M., Watanabe, N.,
395 Ashfold, M. N. R., and Looock, H.-P.: Measurements of energy partitioning in H₂
396 formation by photolysis of amorphous water ice, *Astrophys. J. Lett.*, 682, L69, 2008b.

397



398

399

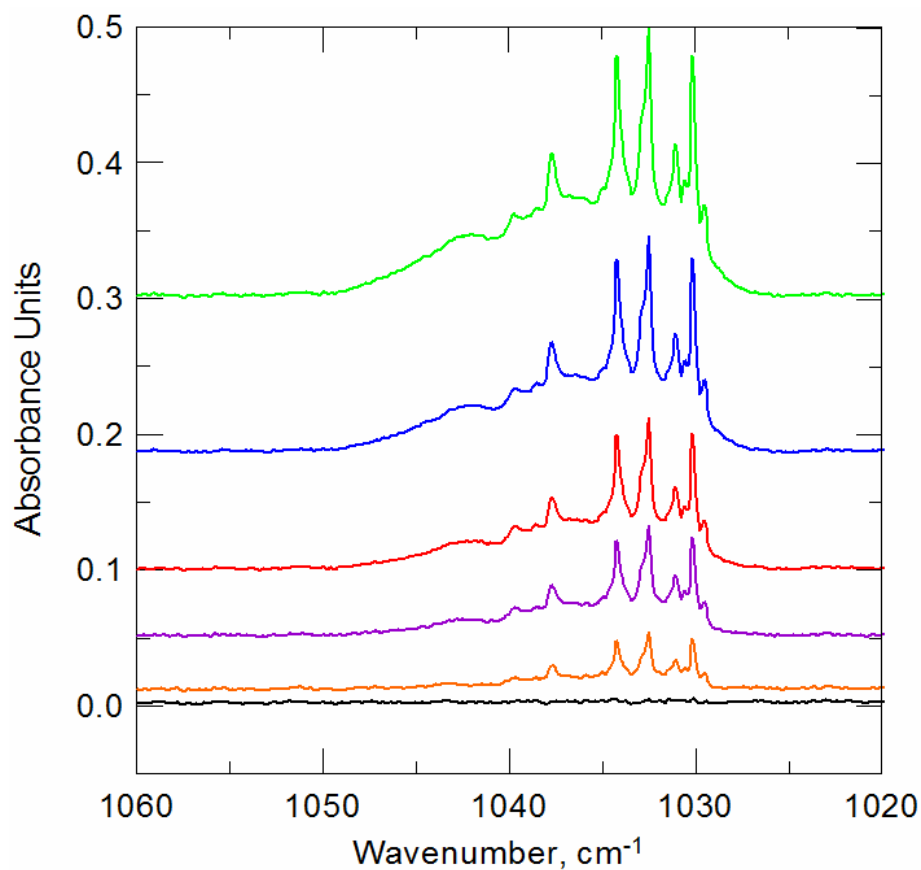
400

401

402

403

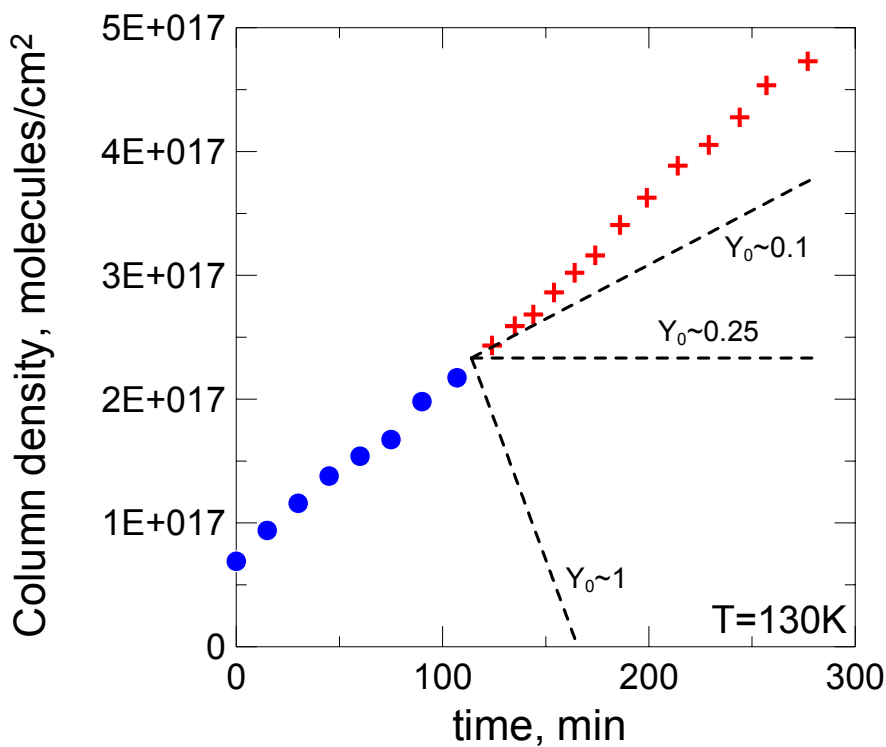
404 **Figure 1.** Scheme of the laboratory setup illustrating the preparation of the ice film
405 sample, its irradiation with VUV light by means of a hydrogen lamp and the
406 measurement of IR spectra in the RARS mode.



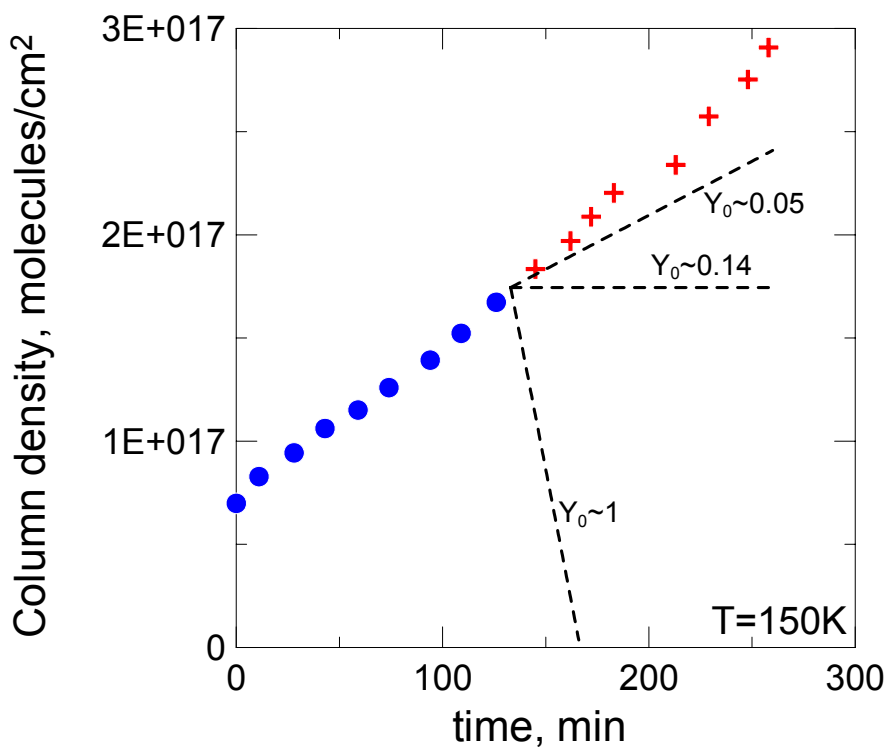
407

408

409 **Figure 2.** Absorption spectra of solid molecular oxygen at T=16 K before irradiation
 410 (black line) and after 1 min (orange), 6 min (purple), 16 min (red), 26 min (blue) and
 411 79 min (green) of irradiation with the resonance hydrogen lamp (at a microwave
 412 generator power output of 30 W) showing the growth of the O₃ band multiplet in the
 413 1040 – 1030 cm⁻¹ range.



414



415

416

417 **Figure 3.** Time evolution of column density at different temperatures before
 418 irradiation (blue points) and after switching on VUV lamp (red crosses). The dashed
 419 black lines indicate asymptotic trends of the column density corresponding to
 420 different theoretical values of absolute photodesorption yield (in molecule/photon).